

Deep Partial Least Squares for IV Regression

Maria Nareklishvili
Booth School of Business
University of Chicago

Nicholas Polson*
Booth School of Business
University of Chicago

Vadim Sokolov
Department of Systems Engineering
and Operations Research
George Mason University

July 7, 2022

Abstract

In this paper, we propose deep partial least squares for the estimation of high-dimensional nonlinear IV regression. As a precursor to a flexible deep neural network architecture, our methodology uses partial least squares (PLS) for dimension reduction and feature selection from the set of instruments and covariates. A central theoretical result, due to Brillinger, shows that the feature selection provided by PLS is consistent and the weights are estimated up to a proportionality constant. We illustrate our methodology with synthetic datasets with a sparse and correlated network structure, together with and draw applications to the effect of childbearing on the mother's labor supply based on classic data of [Angrist and Evans \(1996\)](#). The results on synthetic data as well as applications show that the deep partial least squares method significantly outperforms other related methods. Finally, we conclude with directions for future research.

1. Introduction

Nonlinear IV regression plays an important role in estimation of the causal effect of an exposure to some outcome. Almost all valid causal inference techniques can be viewed as

*Email: ngp@chicagobooth.edu

applications of instrumental variables (IV) e.g. randomized clinical trials (perfect instrument), random assignment of incentives (intent to treat), natural experiments, regression discontinuity (Heckman, 1995). Current research has focused on deep learning (narrow deep neural nets). The set of basis functions are “self-featurizing” in the sense that feature extraction (dimension reduction) is part of the pattern matching algorithm. The caveats include lack of theory, uncertainty quantification and probabilistic reasoning. We propose deep partial least squares as one methodology to address these issues. One can view our approach as merging two cultures (Monis et al., 2022) of machine learning tools and statistical inference (Brillinger, 2012; Sarstedt et al., 2022). Our approach is unique in that we can find relevant features based on linear methods, such as PLS, and account for the uncertainty in this to form predictors that are ensemble averages of deep learners. Polson and Sokolov (2017) discuss the advantage of deep learners for finding relevant predictors in high-dimensional settings.

Randomized control trials (RCTs) play an important role in determining the relative efficacy of several treatments. For policy makers, RCT can inform about the ranking and effectiveness of various regulatory changes. Due to random selection, RCTs also meet the exchangeability assumption that is needed to consistently infer a causal parameter of interest (McCullagh, 2005). In many settings, however, RCT can be expensive, unethical or impossible to implement. The free choice of an individual to self-select into some treatments can bias the results (Griliches, 1977; Kane et al., 1999). In that case, unobserved omitted variables can determine the outcome variable, and standard tools, such as ordinary least squares (OLS), are biased. The instrumental variable (IV) regression is an attractive econometric tool to capture the causal effect of a given treatment on the outcome of interest. A valid instrumental variable meets the following assumptions: it has a significant effect on the treatment (i.e., relevance). It does not influence the outcome directly, through channels other than the treatment (i.e., the exclusion restriction), and a valid instrument is not associated with the unobserved characteristics that affect the outcome (i.e., exogeneity). Under these assumptions, IV recovers unbiased and consistent coefficients of interest.

In addition to the *endogeneity* issue (Abdallah et al., 2015), prediction becomes particularly challenging when the number of features exceeds the number of observations in the data (McCullagh and Polson, 2018). To deal with the issues, several authors use wide and shallow neural networks in the context of IV regression (Hartford et al., 2016; Liu et al., 2020). Deep skinny neural networks have the advantage of being able to efficiently model variables in high-dimensional settings, commonly encountered in the IV regression. To further enhance the efficiency of the networks, some authors introduce linear methods as a precursor to implementing a deep learning model. Debiolles et al. (2004); Jia et al. (2016) use partial least squares (PLS) to extract features before learning the output with deep neural networks. PLS is a linear method which selects variables from a high-dimensional feature space that are particularly relevant for predicting the outcome.

A traditional approach to estimate the IV regression is a two-stage-least-squares (2SLS) technique. In the first stage, valid instrumental variables predict the treatment. In the second stage, another regression estimates the effect of the predicted treatment (and possibly other control variables) on the outcome of interest (Mogstad et al., 2021). When the relation of the treatment and instruments is nonlinear, Terza et al. (2008) show that the method is inconsistent. Iwata (2001) uses a re-centered and re-scaled outcome variable and proves consistency of the method for censored and truncated data. Terza et al. (2008) and Adkins (2012) use predicted treatment residuals in addition to the treatment and other exogenous variables in the second stage regression. Controlling for residuals in the outcome regression has a long history (Florens et al., 2002; Heckman and Navarro-Lozano, 2004; Navarro, 2010). The methods introduced by Terza et al. (2008); Adkins (2012) can also be identified as control function methods.

Our goal here is to extend deep partial least squares (DPLS) method to efficiently extract relevant instruments in the first stage regression. More importantly, when the observed outcome variables consist of errors, we show that the method consistently identifies coefficients of interest under a re-centered and re-scaled outcome described by Iwata (2001) or after controlling for the predicted residuals in the second stage regression as illustrated by Heckman and Navarro-Lozano (2004). The first layer of DPLS consists of a partial least squares method to extract features via hyperplanes in a high-dimensional setting. The subsequent layers efficiently post-process them based on ReLU networks as a deep learner (Yarotsky, 2017). PLS is an attractive method for feature extraction. However, as an alternative, the generalized method of moments (GMM, Hansen and Singleton, 1982) can also be applied to our feature selection stage to provide variance stabilised estimators. This results in a statistical improvement on traditional stochastic descent estimators that are commonplace in machine learning (see, for example, Iwata and Ghahramani, 2017).

Statistical properties of deep neural networks are sparse but growing. Polson and Ročková (2018) discuss theoretical foundations of sparse ReLU networks and the advantage of using Spike-and-Slab prior as an alternative to Dropout. They show that the resulting posterior prediction of ReLU networks with Spike-and-Slab regularization converge to a true function at a rate of $\log^\delta(n)/n^{-K}$ for $\delta > 1$ and a positive constant K . Polson and Sun (2019) provide a theoretical connection between the Spike-and-Slab priors and L_0 norm regularization. They demonstrate that the regularized estimators can result in improved out-of-sample prediction performance. To emphasize the advantages of regularization in deep neural networks, Bhadra et al. (2020) discuss theoretical and empirical justifications (as well as challenges) for the horseshoe prior.

By comparison, Hanin and Rolnick (2019) derive the sharp upper bound for the number of activation function regions in ReLU neural networks. They find that this number in practice is far from the maximum possible and depends on the number of neurons in the network, rather than the depth. A recent paper by Farrell et al. (2021) provides

groundbreaking results on the asymptotic theory of deep neural networks. Under the assumption that the number of hidden layers, i.e., the depth of the network, grows with the sample size, they provide a high probability convergence rate for ReLU neural networks.

Our paper sheds light on the dimension reduction importance in sparse ReLU networks. Specifically, DPLS provides a simple, interpretable framework for reducing a high-dimensional instrumental variable space when the policy (treatment) and outcome are measured with errors. DPLS consists of the system of equations that can theoretically be viewed as an infinite sequential generalization of 2SLS. Beyond the consistency of this method, we demonstrate that the shrinkage in the first layer can substantially improve prediction performance in a traditional high-dimensional instrumental variable regression.

To illustrate prediction performance of DPLS in the IV regression, we design two simulation experiments. The first simulation setup considers a high-dimensional instrumental variable space, where a few of them are redundant for predicting the treatment. In this setup, instruments are uncorrelated with each other. The second simulation design extends the first one by introducing a network structure among instruments (Jeong et al., 2003). In this setup, instruments are sparsely correlated, and a few of them are not related to the treatment. We also demonstrate prediction performance on data provided by Angrist and Evans (1996). The instruments consist of a mixed-sex preference of parents and its' interactions with parental characteristics that are relevant for predicting the mother's labor supply. In each design, we show that DPLS can substantially improve upon benchmark methods. In particular, simulation experiments show that the first stage prediction performance improvement of DPLS relative to OLS, LASSO (Tibshirani, 2011) and DeepIV (Hartford et al., 2016) is more than 79%, 57% and 22%, respectively. More importantly, we find that PLS and LASSO result in similar prediction performance in terms of R^2 and the mean squared error. However, a deep, multi-layered structure of PLS significantly increases predictive performance and the representation learning ability. To incorporate uncertainty of the model coefficients, we also consider the extension of DPLS to a Bayesian framework, and discuss implications.

One area for future research is the study of full uncertainty quantification. It is well known that posterior distributions for IV regression require careful assessment dating back to Zellner (1975) (see also Hoogerheide et al., 2007; Lopes and Polson, 2010). Puelz et al. (2017) discuss parameter uncertainty and variable selection in linear factor models. Hahn et al. (2020) provide a fully Bayesian model for posterior uncertainty for causal inference using Bayesian Additive Regression Trees (BART) to model the nonlinearity in the outcome equation. This provides a gold-standard for comparison to a Bayesian DPLS method.

The rest of the paper is outlined as follows. Section 2 describes our general nonlinear IV model and specific Tobit variation. In section 3 we discuss dimensionality reduction with partial least squares. In Section 4 we introduce deep partial least squares and examine asymptotic theory. Section 5 illustrates applications of the method. Finally, Section 6

concludes with directions for future research.

2. Nonlinear IV Model

One goal is to predict the outcome y^* that possibly nonlinearly depends on a policy (treatment) p^* and high-dimensional x for each observation $i = 1 \dots, n$:

$$y^* = f(p^*\beta + x\beta_x) + u. \quad (2.1)$$

We assume, neither y^* nor p^* are directly observable. Instead, they consist of errors. Define the following variables

- $(y^*, y) \in \mathbb{R} =$ the potential and observed outcome variables,
- $(p^*, p) \in \mathbb{R} =$ the potential and observed policy variables,
- $x \in \mathbb{R}^k =$ observable features,
- $z \in \mathbb{R}^m =$ instrumental variables,
- $(u, w, v, \varepsilon) \in \mathbb{R} =$ latent/error variables that affect (y^*, p^*, p, y) , respectively.

Instead of (2.1), we have access to the following structural equation model:

$$\begin{aligned} p &= p^* + v, \\ p^* &= g(z\alpha + x\alpha_x) + w, \\ y &= \tau(y^*) + \varepsilon. \end{aligned} \quad (2.2)$$

$f(\cdot)$ and $g(\cdot)$ are potentially non-linear continuous functions, possibly deep learners (Hartford et al. 2016). $\tau(\cdot)$ is a known transformation. In this study, we define the Tobit model $\tau(y^*) = 1(y^* > 0) \cdot y^*$. The error v is assumed to be uncorrelated with any other latent error. However, policy p^* is allowed to correlate with u . Covariates x can be high-dimensional and are typically independent of w, v and u . β and β_x represent the effects of p^* and x on y , while α and α_x are the effects of instruments z and covariates x on the policy p^* , correspondingly. The errors w and u are correlated. For example, consider, y is a customer's decision to buy an airline ticket (observed for a particular group of customers), and p^* is the price of this ticket. In that case, policy p^* is said to be endogenous when, conditional on x , (p^*, u) correlate. i.e, $\mathbb{E}(u|x, p^*) \neq 0$. For example, ticket prices might increase during conferences which are unobservable to a researcher, and in that case, $\mathbb{E}(p^*u|x) \neq 0$. Classical estimation methods will lead to a spurious positive relation of prices and sales.

Define the joint error $\eta = w + v$. Moreover, without the loss of generality, assume f is an identity link. Then by replacing p^* with p in (2.1) and combining (2.1) and (2.2), we get:

$$\begin{aligned} y &= \tau(p\beta + x\beta_x + u) + \varepsilon, \\ p &= g(z\alpha + x\alpha_x) + \eta, \end{aligned} \tag{2.3}$$

where the latent errors u and η are correlated through w . The structural equation model in (2.3) defines the nonlinear IV framework. In a traditional nonlinear IV setup (when $\tau(\cdot)$ is an identity function), the presence of valid instruments z that satisfy Assumptions 1-3 allows us to predict the unbiased mean outcome.

Assumption 1 (Relevance). *Instruments z strongly relate to policy p , i.e., the density of p , $F(p|z, x)$, is not constant in z .*

Assumption 2 (Exclusion Restriction). *z is conditionally orthogonal to outcome y :*

$$z \perp y \mid (x, p, u).$$

Assumption 3 (Exogeneity). *z is conditionally orthogonal to the latent error term u :*

$$z \perp u \mid x.$$

Specifically, when $y = p\beta + x\beta_x + \xi$ with $\xi = u + \varepsilon$, valid instruments efficiently separate information in p that is unrelated to u , and consistently identify the effect of the policy on outcome (β). For example, if fuel costs is an instrument for ticket prices, and uncorrelated with confounders, it can recover the exogenous variation in ticket prices and correctly estimate the negative relation of prices and the ticket sales.

Under Assumptions 1-3, a standard approach to consistently identify β is a 2SLS method. The method entails predicting \hat{p} in the first stage (“treatment network”). Then the predicted policy \hat{p} replaces p in the outcome equation, and we estimate a second stage regression (“outcome network”) with another consistent method (Angrist and Evans, 1996; Hartford et al., 2016; Mogstad et al., 2021).

Consistent outcome prediction in a standard IV regression (where $\tau(\cdot)$ is an identity link) can be useful for policy analysis. Define the predicted mean outcome:

$$\mathbb{E}(y|x, z) = \mathbb{E}[f(p, x)|x, z] + \mathbb{E}[\xi|x]. \tag{2.4}$$

Then we can evaluate the effect of a marginal change in policy (e.g., prices) from p_0 to p_1 on the outcome of interest (treatment effect):

$$\mathbb{E}(y|p_1, x) - \mathbb{E}(y|p_0, x) = \mathbb{E}[f(p_1, x)|x, z] - \mathbb{E}[f(p_0, x)|x, z].$$

The issue is that $\tau(\cdot)$ typically is not an identity function. In such nonlinear regression models, latent errors are no longer additively separable from the true regressors (\hat{p} and u are still related), and hence, the true relationship breaks down with errors in variables. The orthogonality condition of the instruments and the outcome error is violated: $\mathbb{E}(z(y - p\beta)|x) \neq 0$. As a result, the 2SLS estimator fails to be consistent for nonlinear errors-in-variables models (Amemiya, 1985). Moreover, when instruments and/or covariates are high-dimensional and nonlinearly relate to the policy and outcomes, OLS is no longer an efficient solution of (2.3).

The goal in this paper is to consistently predict outcome y^* when z and/or x are high-dimensional. To do so, we extend deep partial least squares with a recentered and rescaled outcome (Iwata, 2001), and additionally illustrate it with a control function approach (Terza et al., 2008).

A. Prediction in Low-Dimensional Data

In this section, we abstract from the fact that z and x are high-dimensional and focus on prediction under a Tobit model $\tau(y^*) = 1(y^* > 0)y^*$. We show that, under a recentered and rescaled outcome, 2SLS can consistently identify β . Alternatively, control function approach can lead to a valid prediction of the outcome.

2SLS with the Tobit Model

Define the rescaled output variable,

$$\tilde{y} = \psi_1^{-1}(y - \psi_2), \text{ where } \psi_1 = \text{cov}(y, y^*)/\text{var}(y^*), \psi_2 = \mathbb{E}(y) - \psi_1\mathbb{E}(y^*).$$

Assume that (y^*, z) have a joint elliptical (or Gaussian in the simplest setting) distribution.

Elliptically contoured distributions have the property that

$$\mathbb{E}(z | y^*) - \mathbb{E}(z) = \gamma(y^* - \mathbb{E}(y^*)).$$

Moreover, elliptical contours allow for discrete outcomes. By Stein's lemma, with $y = \tau(y^*) + \varepsilon$

$$\text{cov}(z, \tilde{y}) = \psi_1 \text{cov}(z, y^*) \text{ where } \psi_1 = \text{cov}(y, y^*)/\text{var}(y^*).$$

Specifically, we can calculate the covariance of instruments and re-scaled output as

$$\text{cov}(z, \tilde{y}) = \psi_1^{-1} \text{cov}(z, y) = \psi_1^{-1} \mathbb{E}_{y^*} (\mathbb{E}((z - \mathbb{E}(z))y | y^*))$$

Conditional expectations are linear under elliptical contours, and $\mathbb{E}(y | y^*) = \tau(y^*)$ gives

$$\begin{aligned} \text{cov}(z, \tilde{y}) &= \psi_1^{-1} \mathbb{E}_{y^*} (\mathbb{E}(\gamma(y^* - \mathbb{E}(y^*))y | y^*)) \\ &= \gamma \psi_1^{-1} \mathbb{E}((y^* - \mathbb{E}(y^*))\tau(y^*)) = \gamma \psi_1^{-1} \text{cov}(y^*, \tau(y^*)) \\ &= \gamma \text{cov}(z, y^*) \end{aligned}$$

2SLS first regresses p on z and x to get the predicted policy \hat{p} . Define $\bar{Z} = [z, x]$ and $\hat{p} = P_z \bar{Z}$ where $P_z = \bar{Z}(\bar{Z}^T \bar{Z})^{-1} \bar{Z}^T$ is the projection matrix onto the instrumental variable space (including covariates). In addition, define $\bar{P} = [\hat{p}, x]$ and let $e = \tilde{y} - p\beta$ be the residual from the re-scaled regression, then

$$\text{cov}(z, e|x) = \text{cov}(z, \tilde{y} - p\beta|x) = \text{cov}(z, y^* - p\beta|x) = \text{cov}(z, u|x) = 0.$$

The re-scaled instrumental variable estimator is given by

$$\hat{\beta}^{GMM} = (\bar{Z}^T P_z \bar{Z})^{-1} P_z \bar{Z}^T \tilde{y} = (\bar{P}^T \bar{P})^{-1} \bar{P}^T \tilde{y} \quad (2.5)$$

From the above, we then have $E(\hat{\beta}^{GMM}) = \beta_p$ with $\beta_p = [\beta, \beta_x]$ and $E(\tilde{y}) = \bar{P}\beta_p$. Note that $\hat{\beta}^{GMM}$ is a $(m+k) \times 1$ vector, where the first element is the policy effect on outcome.

Estimating the Proportionality Constants

In the Tobit case, the constants ϕ_1, ϕ_2 can be calculated theoretically from the model as

$$\phi_1 = \Phi(\delta) \quad \text{and} \quad \phi_2 = \sigma_y^* \phi(\delta)$$

with

$$\delta = \mu_X^T \beta / \sigma_y^* \quad \text{and} \quad (\sigma_y^*)^2 = \sigma_{y^*}^2 + \beta^T \Sigma_{xx} \beta.$$

Iwata (2001) shows that, with the truncated outcome variable, we can obtain their estimators:

$$\begin{aligned} \hat{\psi}_1 &= \hat{\Phi} = \frac{1}{n} \sum_{i=1}^n \mathbb{1}(y_i^* > 0), \\ \hat{\psi}_2 &= \hat{\sigma}_y^* \hat{\phi} \quad \text{where} \quad \hat{\phi} = \phi(\Phi^{-1}(\hat{\psi}_1)). \end{aligned}$$

The estimator of the variance of the outcome variable is given as

$$\hat{\sigma}_y^{*2} = \frac{1}{n c(\hat{k})} \sum_{i=1}^n (y_i^* - \bar{y})^2,$$

where

$$c(\hat{k}) = \hat{\Phi} - (\hat{\phi} - \Phi^{-1}(\hat{\Phi}))(1 - \hat{\Phi})(\hat{\phi} + \Phi^{-1}(\hat{\Phi})\hat{\Phi}),$$

and $\hat{\Phi} = \hat{\psi}_1$ and ϕ are the cumulative and probability density functions of a normally distributed random variable, respectively. Iwata (2001) shows that the scaling constant $\hat{\psi}_1$ and the estimator $\hat{\beta}^{GMM}$ defined in (2.5) are asymptotically jointly normally distributed, with

$$\sqrt{n}(\hat{\psi}_1 - \psi_1) \rightarrow \mathcal{N}(0, \hat{\psi}_1(1 - \hat{\psi}_1)), \quad (2.6)$$

$$\sqrt{n}(\hat{\beta}^{GMM} - \beta) \rightarrow \mathcal{N}(0, \Sigma_* - \Phi(1 - \Phi)\beta\beta^T). \quad (2.7)$$

Based on Hansen and Singleton (1982), Σ_\star is the variance of the standard GMM estimator and can be computed as follows ¹:

$$\begin{aligned}\widehat{\Sigma}_\star &= n(\bar{P}^T \bar{Z} \widehat{G} \bar{Z}^T \bar{P})^{-1} \bar{P}^T \bar{Z} \widehat{G} (n \widehat{A}) \widehat{G} \bar{Z}^T \bar{P} (\bar{P}^T \bar{Z} \widehat{G} \bar{Z}^T \bar{P})^{-1}, \\ \widehat{A} &= \frac{1}{n} \sum_i \widehat{e}_i^2 \bar{Z}_i \bar{Z}_i^T, \quad \text{with } \widehat{e}^2 = \widehat{y} - \bar{P} \widehat{\beta}^{GMM}, \\ \widehat{G} &= \widehat{H} (\widehat{H}^{-1} - \bar{Z}^T \bar{Z} / \bar{Z}^T \widehat{H} \bar{Z}) \widehat{H}, \\ \widehat{H} &= \widehat{A}^{-1}.\end{aligned}$$

B. Control Function Approach

An alternative approach to consistently estimate the parameters is a control function approach. Terza et al. (2008) discuss consistency of the two-stage-residual-inclusion (2SRI) approach. Instead of substituting the predicted policy in the second stage regression, we control for the predicted residuals of the first stage:

$$\widehat{\eta} = p - \widehat{p}, \quad (2.8)$$

$$y = \tau(p\beta + \widehat{\eta}\beta_\eta) + \varepsilon^{2SRI}, \quad (2.9)$$

where the residuals of the treatment network $\widehat{\eta}$ can be predicted by any consistent method. ε^{2SRI} is not identical to ε due to the substitution of u with $\widehat{\eta}$. Control function approach can be viewed as a special case of 2SLS. Specifically, the inclusion of $\widehat{\eta}$ in the outcome equation of (2.3) allows us to control for the correlation of η and u , and predict the outcome consistently.

3. Dimensionality Reduction

The identification of $\widehat{\beta}^{GMM}$ in (2.5) rests on the assumption that the number of instruments (as well as independent variables) is strictly lower than the number of observations. In practice, instruments can be high-dimensional (Belloni et al., 2014) and possibly non-linearly related to the policy variable. In that case, $\widehat{\beta}^{GMM}$ might capture the unwanted variation reflected in the predicted policy \widehat{p} (Gagnon-Bartsch et al., 2013). Since \bar{Z} are independently and identically distributed normal random variables with covariance Σ_{zz} , Brillinger (2012) showed that

$$\text{cov}(\bar{Z}, p) = \text{cov}(\bar{Z}, f(U)) = \text{cov}(p, U) \text{cov}(f(U), U) / \text{var}(U) = k \Sigma_{zz} \alpha, \quad (3.1)$$

¹See also Baum et al. (2003) for the discussion of a GMM estimator for the IV regression.

where $\bar{Z} = [z, x]$, $U = \bar{Z}\alpha_z$ with $\alpha_z = [\alpha, \alpha_x]$, and the constant $k = \text{cov}(f(U), U)/\text{var}(U)$. Based on this result, [Brillinger \(2012\)](#) shows that the OLS coefficient is a consistent estimator of α up to a proportionality constant. In this section, we show that the deep partial least squares has the same property.

C. Partial Least Squares

Partial least squares is a dimensionality reduction method that generalizes and combines features from the principal component analysis and multiple regression ([Abdi and Williams, 2010](#)).

Consider the augmented instrumental variable $\bar{Z} = [z, x]$ with the dimension $n \times (m+k)$, where m and k are the dimensions of instruments and covariates, respectively. More importantly, we allow $m+k$ to exceed the number of observations n . The policy $p = P$ is a $n \times 1$ vector as before. PLS can be summarized by the following relationship:

$$\begin{aligned}\bar{Z} &= TV + F, \\ P &= UQ + E,\end{aligned}\tag{3.2}$$

where T and U are $n \times L$ projections (scores) of \bar{Z} and P , respectively. V and Q are orthogonal projection matrices (loadings). Maximizing the covariance between the augmented instruments and the policy leads to the first PLS projection pair (v_1, q_1) :

$$\begin{aligned}\max_{v, q} & (\bar{Z}v_1)^T(Pq_1) \\ \text{subject to} & \|v_1\| = \|q_1\| = 1.\end{aligned}$$

The corresponding scores are $t_1 = \bar{Z}v_1$ and $u_1 = Pq_1$. It is clear that the directions (loadings) for the policy P and the augmented instruments \bar{Z} are the right and left singular vectors of $\bar{Z}^T P$, respectively. PLS in the next step performs an ordinary regression of U on T , namely $U = T\beta$. Then the next projection pair (v_2, q_2) is found by calculating the singular vectors of the residual matrix $(\bar{Z} - t_1v_1^T)^T(P - T\beta q_1^T)$. Lastly, the final regression of interest is $U = T\beta$ (the tutorial [Geladi and Kowalski \(1986\)](#) contains further details).

The key property of PLS is that it is consistent for estimating parameters of interest even in the presence of nonlinearity via a sequence of covariance calculations. [Fisher \(1922\)](#) first observed this in the Probit regression. [Naik and Tsai \(2000\)](#) show the consistency of PLS based on the result of [Brillinger \(2012\)](#). Another desirable property of PLS is that it has a closed form solution. The PLS estimator of α is given as follows ([Helland, 1990](#); [Stone and Brooks, 1990](#)):

$$\hat{\alpha}^{PLS} = \hat{R}(\hat{R}^T S_{zz} \hat{R})^{-1} \hat{R}^T s_{zp},\tag{3.3}$$

where $\hat{R} = (s_{zp}, S_{zz}s_{zp}, \dots, S_{zz}^{q-1}s_{zp})$ is the $(m+k) \times q$ matrix of the Krylov sequence with a $(m+k) \times (m+k)$ matrix S_{zz} and a $(m+k) \times 1$ vector s_{zp} defined as follows:

$$S_{zz} = \frac{\bar{Z}^T(I - 11^T/n)\bar{Z}}{n-1},$$

$$s_{zp} = \frac{(\bar{Z} - \mathbb{E}(\bar{Z}))^T(P - \mathbb{E}(P))}{n-1},$$

where I is an identity matrix and 1 is a matrix of ones. Intuitively, PLS searches for factors that capture the highest variability in \bar{Z} , and at the same time maximizes the covariance between \bar{Z} and P . If the number of factors equals the dimension of instruments, $q = m+k$, the method is equivalent to OLS (Helland, 1990).

4. Deep Partial Least Squares for IV Regression

A useful generalization of PLS is to consider a deep-layered feed-forward neural network structure:

$$\begin{aligned} \hat{p}^{(1)} &= f(\bar{Z}\hat{\alpha}^{PLS}), \\ \hat{p}^{(2)} &= f(\hat{p}^{(1)}\hat{\alpha}^{(2)}), \\ &\vdots \\ \hat{p}^{(L)} &= f(\hat{p}^{(L-1)}\hat{\alpha}^{(L)}), \end{aligned} \tag{4.1}$$

where $f(z) = \max(z, 0)$ is a ReLU activation function. Note that $\bar{Z} = [z, x]$ as before and $\hat{\alpha}^{PLS}$ is a $q \times 1$ vector where q is the number of PLS factors in the treatment network. To reduce the dimensionality of the instruments, we predict the treatment in the first layer by PLS. The parameters $\alpha^{(\ell)}$ in subsequent layers $\ell = 2, \dots, L$ can be identified by OLS or PLS. The following proposition shows that, up to a proportionality constant, the method consistently estimates α in each layer.

Proposition 1. *Let S_{zz} and s_{zp} converge in probability to Σ_{zz} (the population variance of z) and σ_{zp} (the population covariance of z and p) when $n \rightarrow \infty$. Moreover, let there exist a pair of eigenvectors and eigenvalues (v_j, λ_j) for which $\sigma_{zp} = \sum_{j=1}^M \gamma_j v_j$ (with γ_j non-zero for each $j = 1, \dots, M$). Assume also $\mathbb{E}(|g(U)|) < \infty$ and $\mathbb{E}(U|g(U)|) < \infty$ and $q = M$. Then $\hat{\alpha} = \{\hat{\alpha}^{PLS}, \hat{\alpha}^{(2)}, \dots, \hat{\alpha}^{(L)}\}$ are consistent estimators of α up to a proportionality constant.*

Proof. We follow the approach by Naik and Tsai (2000). Let $\alpha^* = \Sigma_{zz}^{-1}\sigma_{zp}$. Define $R = (\sigma_{zp}, \Sigma_{zz}\sigma_{zp}, \dots, \Sigma_{zz}^{q-1}\sigma_{zp})$. Then, based on the assumption that $S_{zz} \rightarrow \Sigma_{zz}$ and $s_{zp} \rightarrow \sigma_{zp}$ when $n \rightarrow \infty$, we have:

$$\hat{\alpha}^{PLS} \rightarrow R(R^T \Sigma_{zz} R)^{-1} \Sigma_{zz} \alpha^* \text{ in probability when } n \rightarrow \infty.$$

The assumptions $q = M$ and $\sigma_{zp} = \sum_{j=1}^M \gamma_j v_j$ imply that α^* is contained in the space spanned by R . Consequently, $\Sigma_{zz}^{1/2} \alpha^*$ is contained in the space spanned by $R^* = \Sigma_{zz}^{1/2} R$. Therefore,

$$R^*(R^{*T} R^*)^{-1} R^{*T} \Sigma_{zz}^{1/2} \alpha^* = \Sigma_{zz}^{1/2} \alpha^*,$$

and

$$R(R^{*T} R^*)^{-1} R^T \Sigma_{zz} \alpha^* = \alpha^*.$$

Hence, $\hat{\alpha}^{PLS} \rightarrow \alpha^*$. Equation (3.1) implies that $\sigma_{zp} = k \Sigma_{zz} \alpha$, and therefore, $\hat{\alpha}^{PLS} \rightarrow \Sigma_{zz}^{-1} \sigma_{zp} = k \alpha$. This proves that the PLS in the first layer is consistent.

Now, consider the second layer $\ell = 2$. If $\hat{\alpha}^{(2)}$ is estimated by either OLS or PLS, (3.1) directly imply that $\hat{\alpha}^{(2)} = k \alpha$. Next, to run OLS (or PLS) of p on $\hat{p}^{(1)}$, we construct

$$\hat{p}^{(1)} = \max(z \hat{\alpha}^{PLS}, 0) = \max(z k \alpha, 0) = k \max(z \alpha, 0) = k z^{(1)}.$$

The model then becomes

$$\hat{p}^{(2)} = \max(k z^{(1)} k_2 \alpha, 0) = k \cdot k_2 \max(z^{(1)} \alpha, 0) = k^{(2)} z^{(2)}. \quad (4.2)$$

By induction, we can consistently estimate α in each subsequent layer, up to L . See Polson et al. (2021) for the detailed discussion of such a deep learning structure.

Lastly, we note that the consistent estimator of the effect of the treatment on outcome is defined as

$$\hat{\beta}^{GMM} = ((\bar{P}^{(L)})^T \bar{P}^{(L)})^{-1} (\bar{P}^{(L)})^T \tilde{y}, \quad (4.3)$$

where $\bar{P}^{(L)}$ is the augmented treatment $[\hat{p}, x]$ predicted by layer L . Moreover, the predicted outcome $\hat{y} = \bar{P} \hat{\beta}^{GMM}$.

Define \hat{e}^L as the predicted residuals from the treatment network in layer L and consider, $\tilde{p} = [p, \hat{e}^L, x]$. Then, similarly for 2SRI:

$$\hat{\beta}^{GMM} = (\tilde{p}^T \tilde{p})^{-1} \tilde{p}^T y. \quad (4.4)$$

and $\hat{y} = \tilde{p} \hat{\beta}^{GMM}$. ■

D. Prediction and Bayesian Shrinkage

One possible extension of deep partial least squares is a quantification of uncertainty in the density of the outcome. Our probabilistic model takes the form:

$$\begin{aligned} \tilde{y} \mid f, \bar{P} &\sim p(\tilde{y} \mid f, \bar{P}), \\ f &= g(\bar{P} \beta_p) + \varepsilon, \end{aligned}$$

where \tilde{y} is an $n \times 1$ rescaled and recentered outcome variable as before, $\bar{P} = [\hat{p}, x]$ is an $n \times (1 + k)$ augmented (predicted) policy. $\beta_p = [\beta, \beta_x]$ is a $(1 + k) \times 1$ vector of coefficients in the outcome network. Here g is a deep partial least squares method. To estimate parameters in the first layer, the method uses the SIMPLS algorithm (De Jong, 1993). Subsequent layers use the stochastic gradient descent (SGD) method (Bottou, 2012) for optimizing and training the parameters.

The key result, due to Brillinger (2012) and Naik and Tsai (2000), is that β_p can be estimated consistently, up to a constant of proportionality using PLS, irrespective of the nonlinearity of g . Given a specification of g , the constant of proportionality can also be estimated consistently with \sqrt{n} -asymptotics. It is worth noting that typically, standard SGD methods will not yield asymptotically normally distributed parameters. However, they can substantially increase precision of the coefficients of interest.

Suppose that we wish to predict the outcome at a new level \bar{P}^* . Then, we can use the predictive distribution to make a forecast as well as provide uncertainty bounds:

$$y_\star \sim p\left(y \mid g(\bar{P}^* \hat{\beta}_p^{DPLS})\right).$$

The advantage of modelling a probabilistic model is the flexibility and the possibility to incorporate uncertainty in the parameters of interest. We approximate the posterior distribution of $\hat{\beta}^{GMM}$ with its asymptotic distribution based on the Bernstein-Von Mises theorem (see e.g., Van der Vaart, 2000; Bhadra et al., 2019). Define Data = (\tilde{y}, p, z, x) , then the densities $P(\hat{\beta}^{GMM} | \text{Data})$ and $P(\hat{\psi}_1)$ come from a normal distribution with the mean and variance depicted in (2.6). To shrink the effect of redundant instruments in the treatment network, we consider a Ridge regression estimator (Marquardt and Snee, 1975):

$$\hat{\alpha}^{Ridge} = (\bar{Z}^T \bar{Z} + \lambda I_m)^{-1} \bar{Z}^T p. \quad (4.5)$$

However, as pointed out by a referee, this still underestimates the uncertainty due to estimation of $(\hat{\beta}_p^{DPLS}, \hat{\alpha}^{Ridge})$. A fully Bayesian model with a non-uniform prior density of the coefficients can increase the precision of uncertainty bounds.

5. Applications

This section illustrates prediction performance of DPLS-IV relative to benchmark methods. We consider synthetic data with high-dimensional sparse and correlated instruments. Kong and Yu (2018) describe such a setting with gene expression data. To illustrate how well the method captures the complex nonlinear and sparse relation of covariates, our design mimics their setup. In addition to synthetic designs, this section illustrates findings on data provided by Angrist and Evans (1996). Throughout the experiments, we split data into two partitions. To find optimal parameters in each method, we use one sub-sample

(further partitioned into train and validation data), and illustrate prediction performance measures on the other.

E. Sparse Uncorrelated Instruments

The data generating process is summarized by the following structural equation model:

$$\begin{aligned}
 y &= f(p\beta + x\beta_x + u) + \varepsilon, \\
 p &= g(z\alpha + \text{sigmoid}(z^2)\gamma + x\alpha_x) + w, \\
 w; u &\sim \mathcal{N}(0, \Sigma), \\
 \varepsilon &\sim \mathcal{N}(0, \sigma_\varepsilon^2), \\
 z &\sim \mathcal{N}(0, \Sigma_z), \quad x \sim \mathcal{N}(0, \Sigma_x), \\
 \alpha; \alpha_x, \gamma, \beta, \beta_x &\sim \mathcal{N}(0, 1).
 \end{aligned} \tag{5.1}$$

(5.1) holds for each observation $i = 1, \dots, n$, where $n = 1000$. w and u are correlated and jointly normally distributed with a mean vector 0 and a variance-covariance matrix $\Sigma = \begin{pmatrix} 3.000 & -0.087 \\ -0.087 & 0.010 \end{pmatrix}$. In this simulation setup, g and f represent ReLU and LeakyReLU functions (Dubey and Jain, 2019). In addition to a $n \times 50$ matrix of instruments z , the treatment p contains nonlinear transformations of z based on the sigmoid function. To introduce sparsity in the design, out of fifty instruments, ten are redundant. In particular, only forty instruments are relevant for predicting the treatment p . x is an $n \times 25$ matrix of covariates, and 20 of them have no influence on outcome y . Σ_z and Σ_x represent covariance matrices of z and x , respectively. In this setting, the covariance between the instruments is small (0.001) and the features x are uncorrelated.

Figure 1 visualizes predictions of the policy p in the treatment network (Figure 10 in Appendix H shows predicted outcome y). In each case, g and f represent a ReLU function. A visual inspection of Figures 1 and 10 verifies that DPLS-IV results in more accurate predictions relative to the other methods. In this setting, DeepIV is the second-best alternative. According to Figures 1 and 10, predictions of the treatment, \hat{p} , appear to have a higher variability compared to the outcome predictions. This is not surprising, as p contains high-dimensional z in addition to x . Note that, even though prediction performance measures of DeepIV are close to those of DPLS-IV, Table V in Appendix H shows that, compared to DeepIV, DPLS-IV is more robust to functional form changes.

To measure the predictive power of each method, we depict R^2 and the root mean squared error (RMSE) for increasing parameter values of Σ . Figure 2 shows that the results of DPLS-IV are robust to increasing errors and the endogeneity of p reflected in the covariance of the error terms w and u . Additionally, Table I shows that DPLS-IV results in a substantial improvement over OLS, PLS, and LASSO models, and a moderate improvement over DeepIV.

To illustrate the predictive power of DPLS-IV, Figure 3 compares coefficients estimated by the OLS and PLS methods in the treatment network. Parameters estimated by PLS are closer to their true values relative to OLS. Additionally, Figure 4 shows the absolute bias of these parameters. According to Figure 4, the cumulative distribution function of the absolute bias of the parameters recovered by PLS stochastically dominates the ones based on OLS and LASSO. Specifically, smaller values of the absolute bias of the coefficients are more likely under PLS, relative to OLS and LASSO. The sum of the absolute bias is smallest under PLS (14.406) and is followed by Lasso (15.233). OLS leads to the highest value of the sum of the absolute bias (21.610).

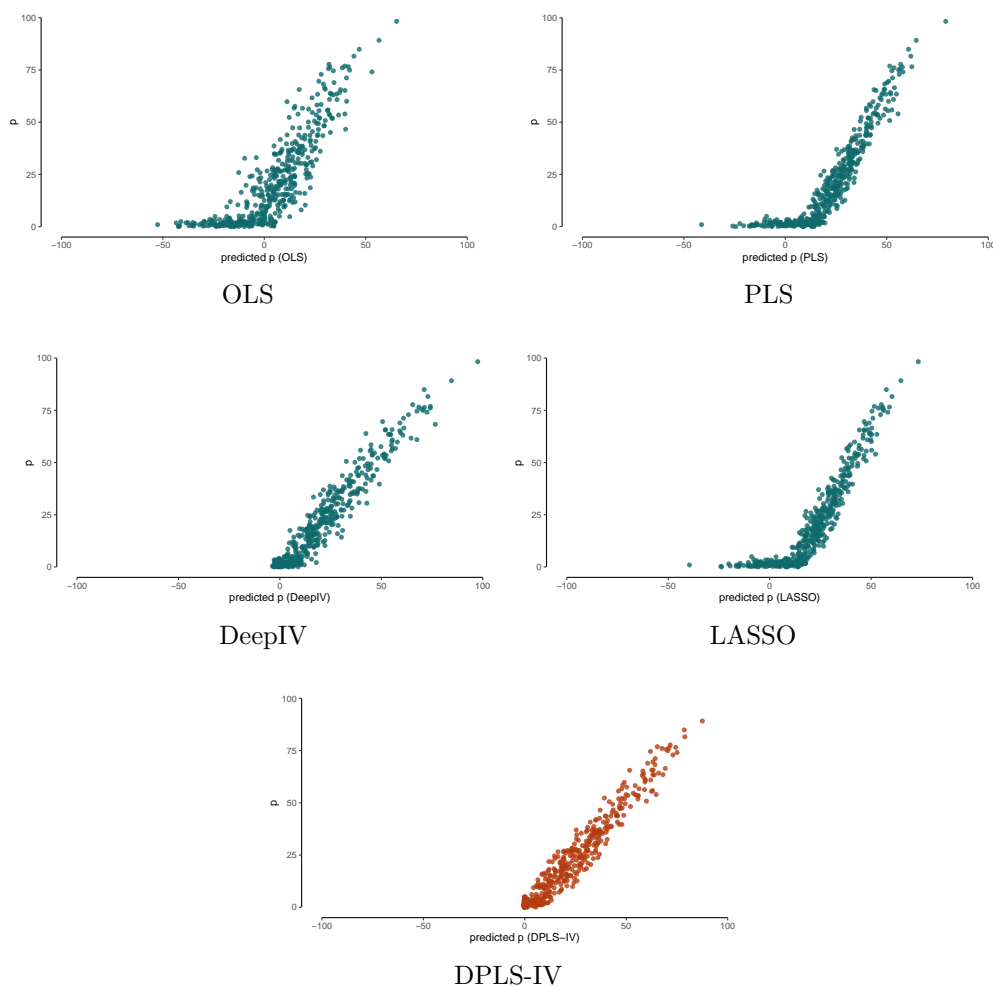


Figure 1. First stage prediction performance. The X-axis depicts predicted treatment \hat{p} , and the Y-axis represents true values of p . DPLS-IV denotes the method introduced in this study. We use test data for evaluating the methods.

Table I. Prediction performance of DPLS-IV relative to other methods. We present out-of-sample R^2 and RMSE. To present the maximum prediction performance of OLS, PLS and LASSO in the outcome network, we use residuals predicted by DPLS-IV in the first stage.

Treatment network					
Measures	PLS	OLS	DeepIV	LASSO	DPLS-IV
R^2	0.751	0.688	0.932	0.753	0.956
RMSE	10.603	21.540	5.789	10.497	4.508
Outcome network					
R^2	0.932	0.933	0.889	0.933	0.938
RMSE	1.668	1.718	4.573	1.670	1.622

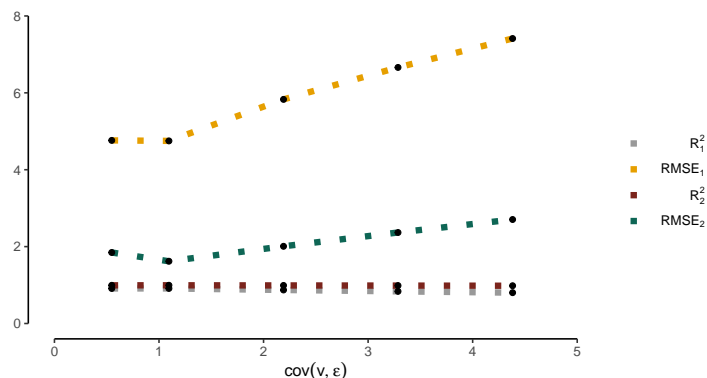


Figure 2. R^2 and RMSE for increasing values of $\text{cov}(v, \varepsilon)$. R_1^2 and RMSE_1 denote prediction performance measures in a treatment network. R_2^2 and RMSE_2 are the prediction performance measures in the outcome network.

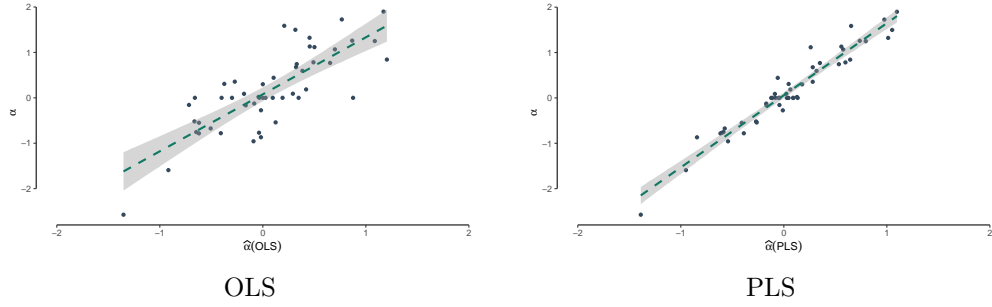


Figure 3. Estimated coefficients and their corresponding true values in the treatment network. The X-axis shows coefficients predicted by OLS (left) and PLS (right), and the Y-axis depicts the corresponding true values.

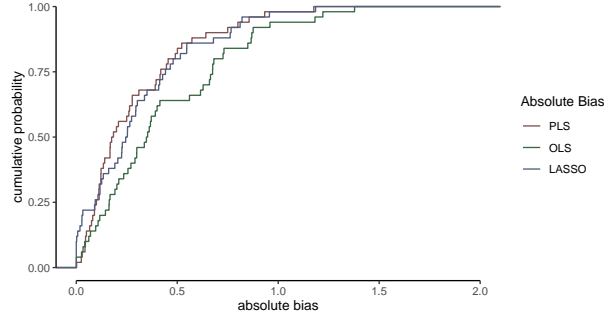


Figure 4. Empirical cumulative distribution functions (CDF) of the absolute bias of the parameters estimated by PLS, OLS and LASSO.

To introduce uncertainty in the parameters of interest, we extend DPLS-IV to a Bayesian setup and compare it to a Bayesian IV approach.

Table II. Prediction performance of Bayesian DPLS-IV and IV methods. The measures are computed based on the mean prediction out of 10,000 predicted outcome variables.

Outcome network		
Measures	Bayesian IV	Bayesian DPLS-IV
R^2	0.778	0.838
RMSE	4.375	3.092

Table II shows that Bayesian DPLS-IV (with ReLU as an activation function and two hidden layers) significantly outperforms its linear counterpart. Figure 5 verifies that the Bayesian DPLS-IV closely replicates the density of the original outcome variable.

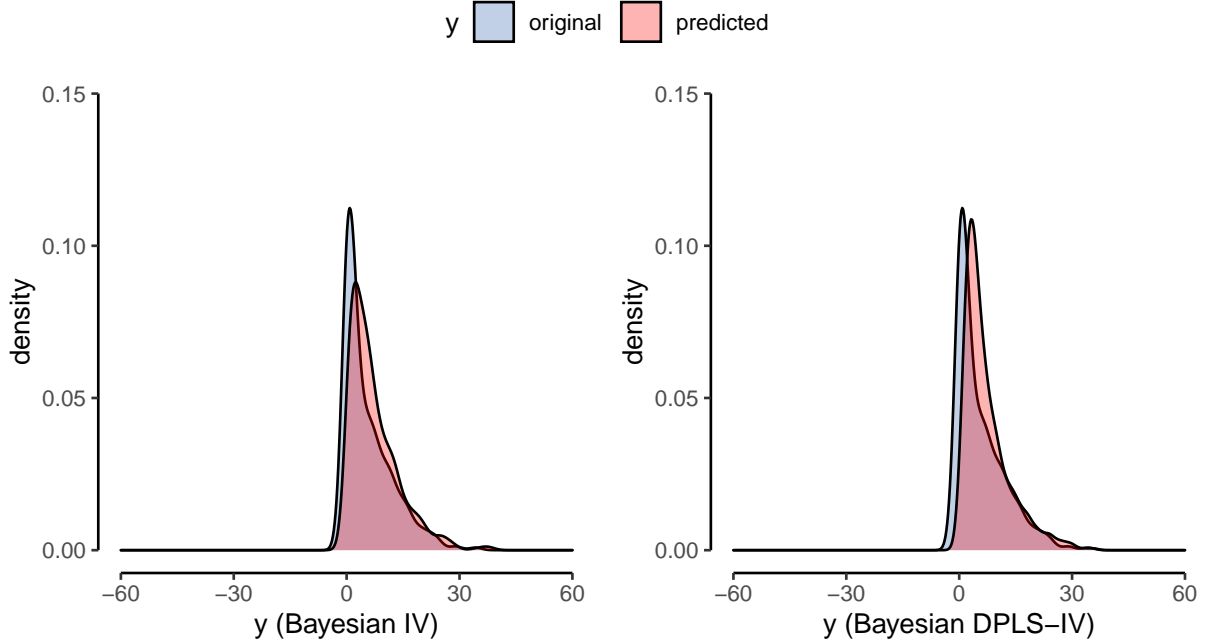


Figure 5. The density of the original and predicted outcome variables (on the test data).

F. Instruments with the Network Structure

The second simulation closely follows the network data structure described by Kong and Yu (2018). The data generating process is the same as shown in (5.1). However, the latent instrumental network comes from the preferential attachment algorithm (Jeong et al., 2003). Each node of the network represents one feature. The resulting network follows a power-law degree distribution, and thus, is scale-free. That means, only a few instruments in the network have relatively large number of “neighbors”. The distance between two instruments is the shortest path between them in the network. We calculate a $p \times p$ ($p = 50$) pairwise distance matrix D . Next, this distance matrix is transformed into a covariance matrix $\Sigma_{z,(i,j)} = 0.7^{D(i,j)}$, where (i, j) represents the element in each row i and column j of a matrix D ($i, j = 1, \dots, p$). Figure 6 shows an example of such a network with 100 nodes.

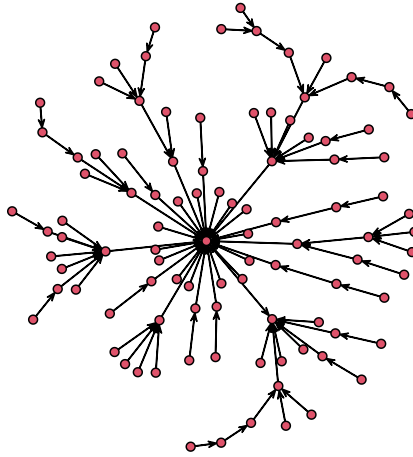


Figure 6. A network with 100 nodes.

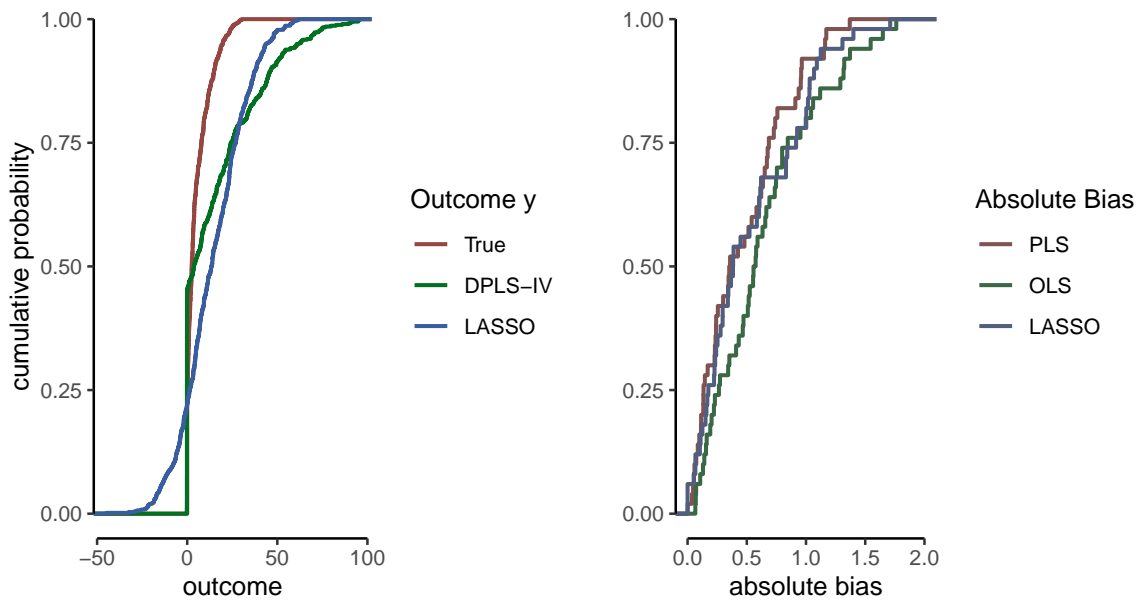


Figure 7. Left - CDF of the outcome variable; Right - CDF of the absolute value of the bias of the parameters (estimated by the corresponding method) in the treatment network.

For comparability, DPLS-IV and DeepIV consist of the same number of layers and neurons in each layer. In particular, the input layer consists of 200 neurons; the hidden layers

consist of 200, 100 and 50 neurons, respectively. We use ReLU as an activation function. Figure 7 shows cumulative distribution functions of the predicted outcome variable and the absolute bias of the estimated coefficients (right) in the treatment network. Based on the results in Figure 7, the outcome predicted by DPLS-IV is closer to CDF of the simulated outcome variable. Moreover, DPLS-IV yields a CDF of the absolute bias of the parameters that stochastically dominates the CDF of the other benchmark methods.

We also investigate prediction performance in the outcome network. Table III shows R^2 and RMSE of DPLS-IV relative to other methods. In this setting, DPLS-IV outperforms other benchmark methods.

Table III. Prediction performance of DPLS-IV relative to other methods. We present out-of-sample R^2 and RMSE. To present the maximum prediction performance of OLS, PLS and LASSO in the outcome network, we use residuals predicted by DPLS-IV in the first stage.

Outcome network					
Measures	PLS	OLS	DeepIV	LASSO	DPLS-IV
R^2	0.940	0.930	0.912	0.942	0.944
RMSE	1.631	1.846	2.108	1.609	1.585

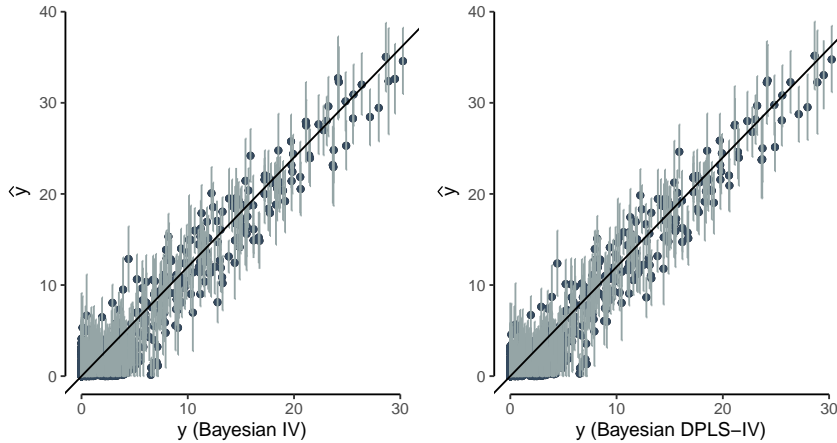


Figure 8. Predicted outcome y and the corresponding 95% confidence intervals.

Additionally, we compare a Bayesian DPLS-IV to a Bayesian IV approach. Bayesian DPLS-IV consists of two hidden layers and a ReLU activation function. Note that, the

RMSE based on the mean predicted outcome out of 10,000 predictions increases (2.262) relative to DPLS-IV. However, R^2 is unchanged (0.941). Figure 8 shows predicted outcome values against their true counterparts. Bayesian DPLS-IV leads to outcome predictions that are closer to the true values.

G. Labor Supply of Women

[Angrist and Evans \(1996\)](#) examine the effect of childbearing on women’s labor supply. They use a mixed sibling-sex composition and twins as instruments for the size of the family. To illustrate the method, our analysis uses 1980 U.S. Census data that include all women with two or more children. The model that we are going to estimate is defined by the following structural equation model:

$$\begin{aligned} y &= f(\text{kids} \cdot \beta + x\beta_x + u) + \varepsilon, \\ \text{kids} &= g(\text{twins} \cdot \alpha + \text{twins} \cdot x\gamma + x\alpha_x) + w, \end{aligned} \tag{5.2}$$

where y is the outcome variable and measures the logarithm of hours worked per week by the mother. The outcome is observed when the age of the mother is more than the average age of the mothers in the population. In particular,

$$y = \log(\text{hourswm})\mathbb{I}(\text{agem} > \mathbb{E}(\text{agem})), \tag{5.3}$$

where $\mathbb{I}(\text{agem} > \mathbb{E}(\text{agem}))$ is an indicator variable and equals one if the age of the mother is more than the population mean, and zero otherwise. The treatment, kids, is the number of total kids in a family. twins represents an instrumental variable and equals one if the second and third children are twins, otherwise zero. Additionally, we use interactions of the instrument with covariates, $\text{twins} \cdot x$ as instruments for the number of kids. The covariates include the gender and age of the first and second child, the mother’s age, marital status, race, education, and the age of the mother when she first gave birth. See [Angrist and Evans \(1996\)](#) for the detailed summary of these variables.

Prediction performance advantage of DPLS-IV is also clearly evident in Table IV. The first stage prediction performance of DPLS-IV is similar in each method, however, R^2 (RMSE) is considerably high (low) in the outcome network. It is worth noting that the measures become substantially worse in the outcome network compared to the ones in the treatment network. One of the potential reasons is that the outcome distribution is bimodal. Figure 11 presents the original density of the outcome variable and the density of the outcome predicted by Bayesian DPLS-IV. Figure 11 shows that Bayesian DPLS-IV successfully captures the bimodal nature of the outcome.

Table IV. Prediction performance of DPLS-IV relative to other methods. We present out-of-sample R^2 and RMSE. To present the maximum prediction performance of OLS, PLS and LASSO in the outcome network, we use residuals predicted by DPLS-IV in the first stage.

Treatment network					
Measures	PLS	OLS	DeepIV	LASSO	DPLS-IV
R^2	0.204	0.205	0.226	0.205	0.233
RMSE	0.655	0.655	0.647	0.647	0.644
Outcome network					
R^2	0.532	0.536	0.771	0.536	0.772
RMSE	12.838	12.782	8.980	12.780	8.960

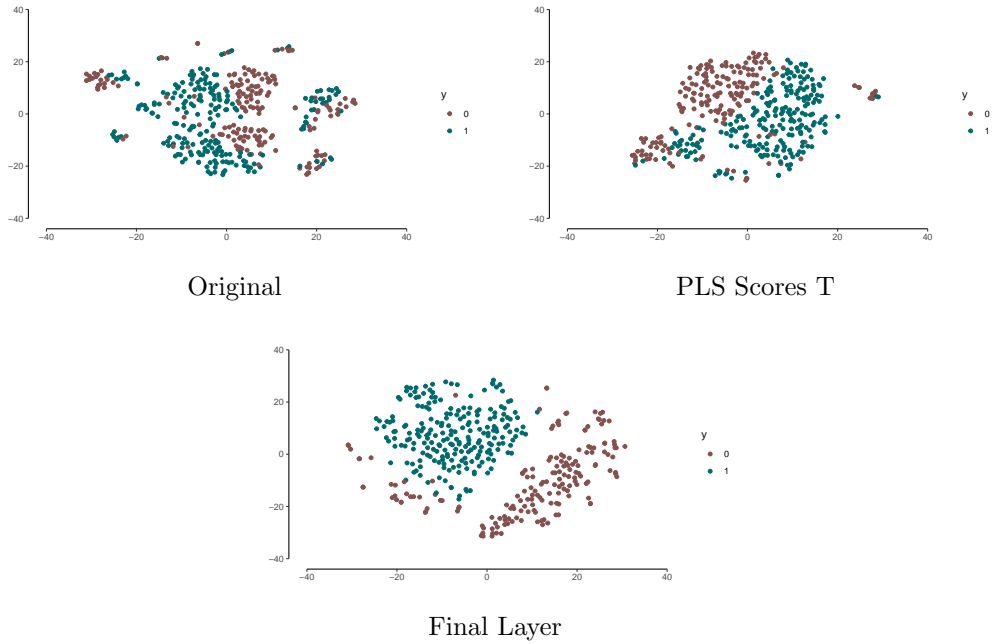


Figure 9. Feature representation of DPLS-IV based on the t-SNE algorithm (with the perplexity parameter equal to 50). Features are represented on two distinct classes of the outcome y , with a class 1 when $y > 0$, and 0 otherwise. The Final Layer represents predicted y of individual neurons in the last layer of DPLS-IV. For simplicity, we randomly sample 1000 observations from the original data.

To investigate the layer-by-layer transformation of the proposed method, Figure 9 illustrates feature representation of the original outcome y (on the test data), the score matrix (T), and the final feed-forward neural network layer in DPLS-IV. We consider the projection of features on two distinct classes of the outcome variable. In particular, when $y > 0$, we label it as a class 1, and when $y = 0$, it represents a class 0. Figure 9 shows that the intermediate layers in DPLS-IV drastically improve the representation of the original covariate space. The borders of the two classes become highly evident in the last layer of DPLS-IV.

6. Discussion

In this article, we propose deep partial least squares for reducing the dimension of the instrumental variable space. The deep partial least squares method efficiently extracts features based on partial least squares and further processes the input with a feed-forward deep learner. The method is well-tailored for correlated instruments with sparse and nonlinear structures. More importantly, deep partial least squares is consistent, up to a proportionality constant.

The applications on synthetic data as well as the application on the effect of childbearing on the mother’s labor supply (Angrist and Evans, 1996) show that the deep partial least squares outperforms other related methods. Moreover, a flexible number of layers allows us to efficiently capture nonlinearities embedded in the instrumental variable network.

An interesting extension of this work is to consider a Bayesian model with various priors on the coefficients of interest. Datta and Ghosh (2013) consider asymptotic properties of Bayes risk with the horseshoe prior. We believe, investigating through different prior beliefs can result in increased predictive performance of deep partial least squares. Another useful extension is to draw applications to eminent domain with judge characteristics as instruments (Belloni et al., 2012). In addition to prediction problems, consistency of DPLS allows us to address estimation of the treatment effect. In future, we plan to demonstrate precision of the treatment effect and compare it to other benchmark algorithms.

References

- Abdallah, W., Goergen, M., and O’Sullivan, N. (2015). Endogeneity: How failure to correct for it can cause wrong inferences and some remedies. *British Journal of Management*, 26(4):791–804.
- Abdi, H. and Williams, L. J. (2010). Principal component analysis. *Wiley interdisciplinary reviews: computational statistics*, 2(4):433–459.

- Adkins, L. C. (2012). Testing parameter significance in instrumental variables probit estimators: some simulation. *Journal of Statistical Computation and Simulation*, 82(10):1415–1436.
- Amemiya, Y. (1985). Instrumental variable estimator for the nonlinear errors-in-variables model. *Journal of Econometrics*, 28(3):273–289.
- Angrist, J. and Evans, W. N. (1996). Children and their parents’ labor supply: Evidence from exogenous variation in family size.
- Baum, C. F., Schaffer, M. E., and Stillman, S. (2003). Instrumental variables and gmm: Estimation and testing. *The Stata Journal*, 3(1):1–31.
- Belloni, A., Chen, D., Chernozhukov, V., and Hansen, C. (2012). Sparse models and methods for optimal instruments with an application to eminent domain. *Econometrica*, 80(6):2369–2429.
- Belloni, A., Chernozhukov, V., and Hansen, C. (2014). High-dimensional methods and inference on structural and treatment effects. *Journal of Economic Perspectives*, 28(2):29–50.
- Bhadra, A., Datta, J., Li, Y., and Polson, N. (2020). Horseshoe regularisation for machine learning in complex and deep models 1. *International Statistical Review*, 88(2):302–320.
- Bhadra, A., Datta, J., Polson, N. G., and Willard, B. (2019). Lasso meets horseshoe: A survey. *Statistical Science*, 34(3):405–427.
- Bottou, L. (2012). Stochastic gradient descent tricks. In *Neural networks: Tricks of the trade*, pages 421–436. Springer.
- Brillinger, D. R. (2012). A generalized linear model with “gaussian” regressor variables. In *Selected Works of David Brillinger*, pages 589–606. Springer.
- Datta, J. and Ghosh, J. K. (2013). Asymptotic properties of bayes risk for the horseshoe prior. *Bayesian Analysis*, 8(1):111–132.
- De Jong, S. (1993). Simpls: an alternative approach to partial least squares regression. *Chemometrics and intelligent laboratory systems*, 18(3):251–263.
- Debiolles, A., Oukhellou, L., and Akinin, P. (2004). Combined use of partial least squares regression and neural network for diagnosis tasks. In *Proceedings of the 17th International Conference on Pattern Recognition, 2004. ICPR 2004.*, volume 4, pages 573–576. IEEE.

- Dubey, A. K. and Jain, V. (2019). Comparative study of convolution neural network’s relu and leaky-relu activation functions. In *Applications of Computing, Automation and Wireless Systems in Electrical Engineering*, pages 873–880. Springer.
- Farrell, M. H., Liang, T., and Misra, S. (2021). Deep neural networks for estimation and inference. *Econometrica*, 89(1):181–213.
- Fisher, R. A. (1922). On the mathematical foundations of theoretical statistics. *Philosophical transactions of the Royal Society of London. Series A, containing papers of a mathematical or physical character*, 222(594-604):309–368.
- Florens, J.-P., Heckman, J., Meghir, C., and Vytlacil, E. (2002). Instrumental variables, local instrumental variables and control functions. Technical report, cemmap working paper.
- Gagnon-Bartsch, J. A., Jacob, L., and Speed, T. P. (2013). Removing unwanted variation from high dimensional data with negative controls. *Berkeley: Tech Reports from Dep Stat Univ California*, pages 1–112.
- Geladi, P. and Kowalski, B. R. (1986). Partial least-squares regression: a tutorial. *Analytica chimica acta*, 185:1–17.
- Griliches, Z. (1977). Estimating the returns to schooling: Some econometric problems. *Econometrica: Journal of the Econometric Society*, pages 1–22.
- Hahn, P. R., Murray, J. S., and Carvalho, C. M. (2020). Bayesian regression tree models for causal inference: Regularization, confounding, and heterogeneous effects (with discussion). *Bayesian Analysis*, 15(3):965–1056.
- Hanin, B. and Rolnick, D. (2019). Deep relu networks have surprisingly few activation patterns. *Advances in neural information processing systems*, 32.
- Hansen, L. P. and Singleton, K. J. (1982). Generalized instrumental variables estimation of nonlinear rational expectations models. *Econometrica: Journal of the Econometric Society*, pages 1269–1286.
- Hartford, J., Lewis, G., Leyton-Brown, K., and Taddy, M. (2016). Counterfactual Prediction with Deep Instrumental Variables Networks. *arXiv:1612.09596 [cs, stat]*.
- Heckman, J. and Navarro-Lozano, S. (2004). Using matching, instrumental variables, and control functions to estimate economic choice models. *Review of Economics and statistics*, 86(1):30–57.
- Heckman, J. J. (1995). Randomization as an instrumental variable.

- Helland, I. S. (1990). Partial least squares regression and statistical models. *Scandinavian journal of statistics*, pages 97–114.
- Hoogerheide, L., Kleibergen, F., and van Dijk, H. K. (2007). Natural conjugate priors for the instrumental variables regression model applied to the angrist–krueger data. *Journal of Econometrics*, 138(1):63–103.
- Iwata, S. (2001). Recentered and Rescaled Instrumental Variable Estimation of Tobit and Probit Models with Errors in Variables. *Econometric Reviews*, 20(3):319–335.
- Iwata, T. and Ghahramani, Z. (2017). Improving output uncertainty estimation and generalization in deep learning via neural network gaussian processes. *arXiv preprint arXiv:1707.05922*.
- Jeong, H., Néda, Z., and Barabási, A.-L. (2003). Measuring preferential attachment in evolving networks. *EPL (Europhysics Letters)*, 61(4):567.
- Jia, W., Zhao, D., and Ding, L. (2016). An optimized rbf neural network algorithm based on partial least squares and genetic algorithm for classification of small sample. *Applied Soft Computing*, 48:373–384.
- Kane, T. J., Rouse, C. E., and Staiger, D. O. (1999). Estimating returns to schooling when schooling is misreported.
- Kong, Y. and Yu, T. (2018). A deep neural network model using random forest to extract feature representation for gene expression data classification. *Scientific reports*, 8(1):1–9.
- Liu, R., Shang, Z., and Cheng, G. (2020). On deep instrumental variables estimate. *arXiv preprint arXiv:2004.14954*.
- Lopes, H. F. and Polson, N. G. (2010). Extracting sp500 and nasdaq volatility: The credit crisis of 2007-2008. *Handbook of Applied Bayesian Analysis*, pages 319–342.
- Marquardt, D. W. and Snee, R. D. (1975). Ridge regression in practice. *The American Statistician*, 29(1):3–20.
- McCullagh, P. (2005). Exchangeability and regression models. *Oxford Statistical Science Series*, 33:89.
- McCullagh, P. and Polson, N. G. (2018). Statistical sparsity. *Biometrika*, 105(4):797–814.
- Mogstad, M., Torgovitsky, A., and Walters, C. R. (2021). The causal interpretation of two-stage least squares with multiple instrumental variables. *American Economic Review*, 111(11):3663–98.

- Monis, J. B., Sarkar, R., Nagavarun, S., and Bhadra, J. (2022). Efficient net: Identification of crop insects using convolutional neural networks. In *2022 International Conference on Advances in Computing, Communication and Applied Informatics (ACCAI)*, pages 1–7. IEEE.
- Naik, P. and Tsai, C.-L. (2000). Partial least squares estimator for single-index models. *Journal of the Royal Statistical Society: Series B (Statistical Methodology)*, 62(4):763–771.
- Navarro, S. (2010). Control functions. In *Microeconometrics*, pages 20–28. Springer.
- Polson, N., Sokolov, V., and Xu, J. (2021). Deep learning partial least squares. *arXiv preprint arXiv:2106.14085*.
- Polson, N. G. and Ročková, V. (2018). Posterior concentration for sparse deep learning. *Advances in Neural Information Processing Systems*, 31.
- Polson, N. G. and Sokolov, V. O. (2017). Deep learning for short-term traffic flow prediction. *Transportation Research Part C: Emerging Technologies*, 79:1–17.
- Polson, N. G. and Sun, L. (2019). Bayesian l₀-regularized least squares. *Applied Stochastic Models in Business and Industry*, 35(3):717–731.
- Puelz, D., Hahn, P. R., and Carvalho, C. M. (2017). Variable selection in seemingly unrelated regressions with random predictors. *Bayesian Analysis*, 12(4):969–989.
- Sarstedt, M., Hair, J. F., Pick, M., Liengaard, B. D., Radomir, L., and Ringle, C. M. (2022). Progress in partial least squares structural equation modeling use in marketing research in the last decade. *Psychology & Marketing*, 39(5):1035–1064.
- Stone, M. and Brooks, R. J. (1990). Continuum regression: cross-validated sequentially constructed prediction embracing ordinary least squares, partial least squares and principal components regression. *Journal of the Royal Statistical Society: Series B (Methodological)*, 52(2):237–258.
- Terza, J. V., Basu, A., and Rathouz, P. J. (2008). Two-stage residual inclusion estimation: addressing endogeneity in health econometric modeling. *Journal of health economics*, 27(3):531–543.
- Tibshirani, R. (2011). Regression shrinkage and selection via the lasso: a retrospective. *Journal of the Royal Statistical Society: Series B (Statistical Methodology)*, 73(3):273–282.
- Van der Vaart, A. W. (2000). *Asymptotic statistics*, volume 3. Cambridge university press.

Yarotsky, D. (2017). Error bounds for approximations with deep relu networks. *Neural Networks*, 94:103–114.

Zellner, A. (1975). Bayesian analysis of regression error terms. *Journal of the American Statistical Association*, 70(349):138–144.

Appendix

H. Prediction Performance Measures with LeakyReLU

Table V. Prediction performance of DPLS-IV relative to other methods. We present out-of-sample R^2 and RMSE. To present the maximum prediction performance of OLS, PLS and Tobit in the outcome network, we use residuals predicted by DPLS-IV in the first stage. We use LeakyReLU to simulate the outcome variables. DPLS-IV consists of an input layer with 50 neurons, and a hidden layer with 30 neurons. DeepIV consists of 100 neurons in the input layer, followed by three hidden layers with 100, 100 and 30 neurons, respectively. We use ReLU to activate neurons in DeepIV and DPLS-IV.

Treatment network					
Measures	PLS	OLS	LASSO	DeepIV	DPLS-IV
R^2	0.757	0.696	0.760	0.939	0.957
RMSE	10.503	21.404	10.398	5.498	4.449
Outcome network					
R^2	0.933	0.933	0.934	0.878	0.938
RMSE	1.666	1.720	1.667	2.224	1.623

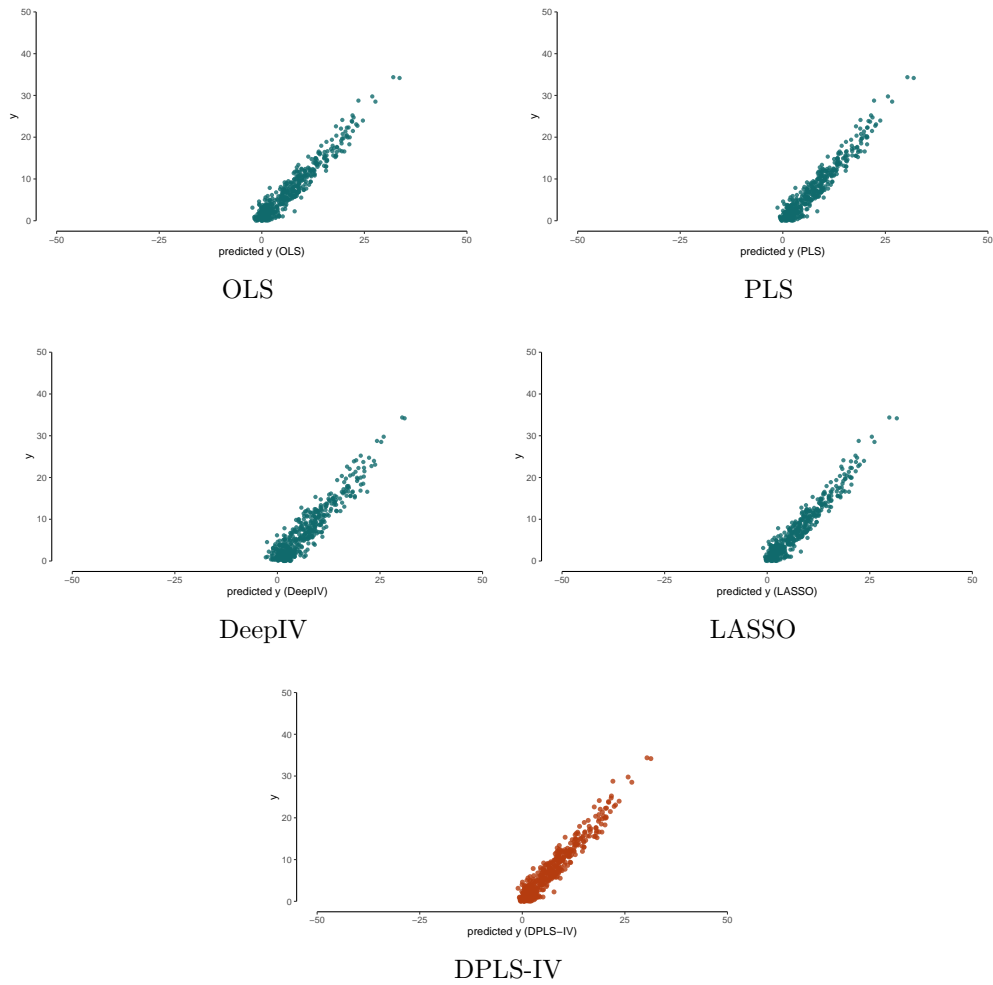


Figure 10. The second stage prediction performance. The X-axis depicts predicted outcome \hat{y} , and the Y-axis represents true values of y . DPLS-IV denotes the method introduced in this study. We use test data for evaluating the methods.

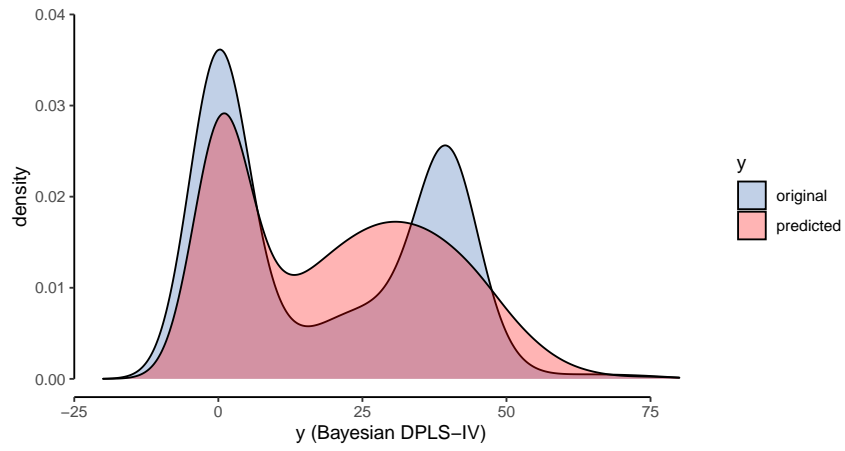


Figure 11. The original distribution of the outcome variable and the one predicted by Bayesian DPLS-IV. Bayesian DPLS-IV consists of two hidden layers and a ReLU activation function.